Cancer Nano (2013) 4:117–125
DOI 10.1007/s12645-013-0044-5

ORIGINAL PAPER

Intelligent system design for bionanorobots in drug delivery

Mark Fletcher · Mohammad Biglarbegian · Suresh Neethirajan

Received: 22 April 2013 / Accepted: 2 July 2013 / Published online: 14 July 2013

Abstract A nanorobot is defined as any smart structure which is capable of actuation, sensing, manipulation, intelligence, and swarm behavior at the nanoscale. In this study, we designed an intelligent system using fuzzy logic for diagnosis and treatment of tumors inside the human body using bionanorobots. We utilize fuzzy logic and a combination of thermal, magnetic, optical, and chemical nanosensors to interpret the uncertainty associated with the sensory information. Two different fuzzy logic structures, for diagnosis (Mamdani structure) and for cure (Takagi–Sugeno structure), were developed to efficiently identify the tumors and treat them through delivery of effective dosages of a drug. Validation of the designed system with simulated conditions proved that the drug delivery of bionanorobots was robust to reasonable noise that may occur in the bionanorobot sensors during navigation, diagnosis, and curing of the cancer cells. Bionanorobots represent a great hope for successful cancer therapy in the near future.

Keywords Bionanorobot · Control system · Drug delivery · Fuzzy logic · Nanomedicine

M. Fletcher · S. Neethirajan
Biomedical Engineering, University of Guelph, Guelph, Ontario, Canada

M. Biglarbegian
Mechanical Engineering, University of Guelph, Guelph, Ontario, Canada

S. Neethirajan (✉)
BioNano Laboratory, School of Engineering, University of Guelph, 50 Stone Road East, Guelph, Ontario N1G 2W1, Canada
e-mail: s.neethi@uoguelph.ca

1 Introduction

Nanomedicine is the technology that uses nanoscale or nanostructured materials such as bionanorobots in medicine that according to their structure have unique medical effects (Wagner et al. 2006). A nanorobot is a smart structure that is capable of intelligent behavior such as actuation, sensing, signaling, information processing, manipulation, and swarm behavior at the nanoscale. Bionanorobots are nanorobots designed and inspired by harnessing properties of biological materials such as peptides and DNAs (Freitas 2006). Bionanorobots present multiple clinical uses including targeted drug delivery, nanosized hybrid therapeutics (low dosage), and early diagnosis at the cellular level (Zhou and Wang 2011). Bionanorobots present a great hope for the treatment of many diseases and conditions including cancer, AIDS, and diabetes. This emerging technology for drug delivery is based on the synergy between several disciplines including biology, chemistry, physics, engineering, and computer science. The first uses of nanorobots in healthcare are expected to be developed within the near future and could have a wide range of biomedical applications (Cavalcanti et al. 2008a; Zhou and Wang 2011).

The potential use of bionanorobots for drug delivery in cancer treatment has multiple advantages over current chemotherapy and radiation techniques. When chemotherapy drugs are ingested or injected, the drug travels throughout the body targeting fast growing cells such as cancer cells and other healthy fast growing cells. This can cause degenerative health effects (Cavalcanti et al. 2008a) such as damage to the digestive tract and heart as well as unfavorable side effects such as hair loss. The damaging side effects limit the dose of the drug administered effectively reducing the amount of the drug that reaches the tumor. In a targeted drug delivery system, the drugs are given directly to the tumor cells that are identified by the bionanorobots. This would reduce the negative side effects and improve the patient's quality of life

during and after the treatment (Cavalcanti et al. 2008b; Karan and Majumder 2011). In addition, the dose of the drug that reaches a tumor cell can be controlled and even increased because of the reduced risk of harmful side effects.

Due to the differences in material and the range of scale, the design and control techniques of bionanorobotics are distinctly different than that of macro robotics. It is imperative to note that the actual environment surrounding the bionanorobot inside the human body is a world of viscosity, where friction, adhesion, and viscous forces play a significant role, while the gravitational force is negligible. The turbulence is not present in the fluid stream due to low Reynolds number. However, fluid shear stress is a major factor that could hamper the bionanorobot due to the robot's traveling speed and the nanoscale size. The challenges associated with the deployment of bionanorobots inside the human body for drug delivery and other medical applications include loop control (Cavalcanti and Freitas 2005) and guidance at the nanoscale and wireless communication for the data transfer (Cavalcanti et al. 2006), accurate modeling of tracking behavior, and power generation at the nanoscale. Some suggested tools for the control of bionanorobots in literature include fuzzy logic, artificial intelligence, and neural networks (Cavalcanti et al. 2004). As such, there are no established set of guidelines currently available detailing the methods of designing and navigating a bionanorobot efficiently inside the human body.

In the aorta, which is the largest artery coming from the heart, the averaged velocity is 33 cm/s. This value depends on the diameter of the blood vessels, blood density, blood viscosity, and relevant parameters. In capillaries, the average velocity is around 0.3 mm/s. At normal conditions, the blood flow velocity (Elad and Einav 2003) in the aorta is between 3 and 5 m/s, while in large arteries it is about 7 and 10 m/s, and in small arteries it is 15 and 35 m/s. The traveling speed of the bionanorobots will rely on the blood flow velocity. Flagellar motors allow bacteria to move at a speed up to 140 μm/s (Neethirajan et al. 2012) with directional reversals occurring approximately 1/s. Based on the results of our nano-porous microfluidic platform-assisted chemotaxis experiments of measuring bacterial velocity, and the nanoscale imaging of the flagellar motor using atomic force microscope, we estimate that the speed (Neethirajan et al. 2012) of bionanorobot will be in the range of 25 to 140 μm/s. The speed will depend on the size of the robot and the number of sensor components and its architecture.

Lymphoma and leukemia are the most common types of blood cancer cells of the human biological system. Leukemia is a cancer of the bone marrow or blood cells while lymphoma is a cancer that starts in the lymphatic system or in the lymph nodes. These two types of cancer may appear similar in size or shape most of the time and may even have similar chemical signatures. The similarity between lymphoma and leukemia tumors, possibilities in inaccurate measurements, and overlap of the thermal, magnetic, and chemical properties surrounding the malignant and beneficial tumor cells and the ever changing environment of the human body can cause a lot of uncertainty inside the human body. An incorrect diagnosis and treatment will not eradicate the cancer but may cause additional harm, which is why it is important for the bionanorobots to be able to handle uncertainty. The reasons for using fuzzy logic system in assisting the bionanorobot towards navigation and drug delivery is twofold: (1) The uncertainty in sensory reading that exists in real life as well as the recommended drug dosages often expressed in a range (as opposed a fixed number) can be interpreted efficiently and (2) it would be possible to design and fabricate the complex structure of bionanorobot by combining multiple rules to handle the sophisticated environments. The motivation for developing the fuzzy control system includes the need for precise control of drug delivery for the two therapeutic agents (doxorubicin and cyclosporine), if both are present in surplus.

2 Development of intelligent system

In clinical treatment, the use of bionanorobots will be done with intravenous injection (Cavalcanti et al. 2008b; Elad and Einav 2003). This method releases the robots directly into the patients' bloodstream. Bio-actuation mechanisms of the bionanorobots will facilitate swimming and swarming behavior inside the blood vessels. A bionanorobot needs to travel through the bloodstream to reach its target, i.e., tumorous cell. Blood contains components such as thrombocytes, leukocytes, erythrocytes, and plasma, and hence, the robot will experience a cluttered and unstructured environment during this traveling process. A major task for a bionanorobot is to efficiently maneuver itself to the malignant tumor cells. To do so, the robot must be equipped with sensors to clearly detect the environment, find its path, and avoid obstacles. More importantly, the robot should recognize the healthy and malignant tumor cells and clearly differentiate them. Due to the sensor noise, uncertainty, and unknown parameters, accomplishing these tasks is challenging mainly because of the robot's ability to effectively handle the uncertain information during decision making such as distinguishing between malignant tumors and beneficial cells, differentiating lymphoma and leukemia type tumor cells, and determining the amount of drug dosage to be delivered.

A bionanorobot (Fig. 1) is made of (a) sensors and (b) an on-board controller to fulfill its mission. It is possible to prototype bionanorobots with multiple sensors (Lenaghan et al. 2013) and nano-actuators (Ghaffari et al. 2012) using molecular dynamics simulation and DNA or peptides

(Hamdi and Ferreira 2008). With regards to the sensors, a temperature sensor or a thermistor, flexi force sensor, photodiode, strain gauge, and a magnetometer are used that allow the robot to make a new trajectory planning decision, identify the obstacles, and distinguish healthy and malignant cells. The bionanorobot relies on the sensors to detect and search the tumor cells using intelligent algorithms. Increased temperature in a zone or regional hyperthermia is related to non-neurological vasodilation and angiogenesis inside the tumor (Zhang et al. 2008). In the human body, temperature changes and generally increases in the inflamed tissues and the area surrounding the tumor cells. The temperature can be up to 2 °C higher for a malignant tumor (McDevitt et al. 2001). This property makes temperature an effective indicator for diagnosing tumors at the nanoscale range. So, a sudden or significant change in temperature occurring every time is an indicator (Zhang et al. 2008) for the robot to identify the malignant tumor cells. The robot's thermal sensor will measure the temperature and make the decisions accordingly. While the movement of the robot will be mostly in a linear fashion, it will also be able to scan all directions by taking a circular fashion using the movement of the cameras/photodiodes of the parts of the robot. In addition to sensors, a bionanorobot will also have a nano-controller on the board to collect the sensory data and make intelligent decision accordingly. To be able to swim in the biological body fluids in the narrow channels and to avoid trapping inside the 4-μm retinal capillaries or the 1- to 2-μm splenofenestral slits, the bionanorobot will be designed with helical flagella (Fig. 1) propellers (Subramanian et al. 2009). Upon successful delivery of the drugs, this flagella propeller crawling mobility of the bionanorobot will facilitate the transport through the excretory system for removal from the blood through either the liver or kidney system.

Cells and tissues in the human body give off measurable electromagnetic impulses. Both cancer and normal cells possess the ability to utilize electromagnetic fields. The structure, size, and the metabolic profiles of cancer cells do not allow utilizing the electrical property in the same fashion as normal cells. The electrical potential of the cell membrane of cancer cells is lower with disrupted electrical connections than the healthy cells (Gonzalez et al. 2012). Frohlich's theory of coherent excitation (Frohlich 1983) and the change in the generation of endogenous electromagnetic field caused due to the vibrations in electrical polar structures (Pokorny et al. 2008) surrounding the cells hypothesize that magnetic property could be effectively used as a method for discriminating between normal tissue and malignant tumors. Bionanorobots can be designed to detect the difference in the electromagnetic field between the cancer and healthy cells. As per the law of magnetic force, the nearby healthy cell may attract the nanorobot compared to a distant cancer cell which might result in a false call. Hence, magnetic property alone

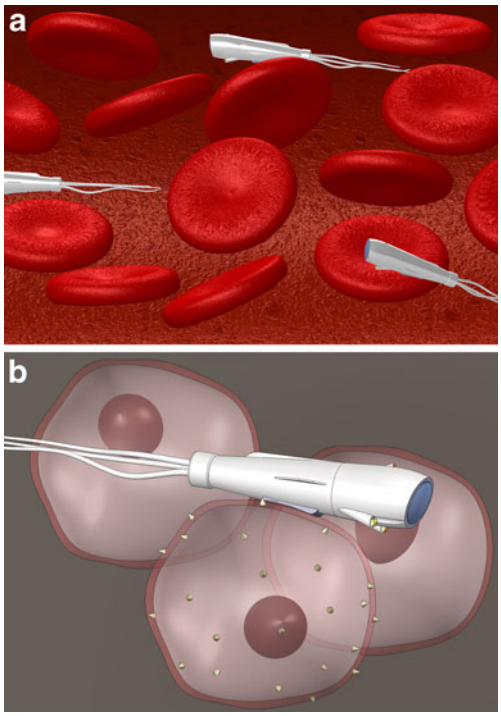

Fig. 1 **a** Schematic illustration of the bionanorobots manoeuvering inside the blood vessel. **b** Bionanorobot's drug delivery to the tumor cell through attachment on the cell surface

cannot be used by the bionanorobot for identifying cancerous cells. When the magnetism and temperature-determined thresholds are exceeded, the bionanorobot will attach to the cell and take a pH (chemical signature) reading. The pH of human blood (Waugh and Grant 2004) is slightly alkaline, ranging from 7.35 to 7.45. As the tumor cell population grows, the oxygen in the surrounding tissue is used up. As anaerobic conditions develop, lactic acid begins to build up as a by-product of the hydrolysis of ATP. This may effectively lower the pH value, and therefore, the pH of the area surrounding the cell can be used for identifying tumors. Hence, an integrated approach of incorporating temperature measurement along with magnetic and chemical (protein expressions or pH) sensing will be an ideal method for the bionanorobots for effective diagnosis of malignant tumors.

When a tumor cell has been identified and the bionanorobot has attached to the cell, it must then correctly diagnose the cancer before it can treat it effectively. Cancer antigen or carbohydrate antigens 125 (CA125) and 19-9 (CA19-9) are glycoprotein molecules that are expressed on the surface of tumor cells. By identifying the concentrations of these markers, the bionanorobot can determine the type of cancer present. An elevated level of CA125 markers suggests the tumor is lymphoma and above normal levels of CA19-9 suggests it is leukemia. Unfortunately, the diagnosis is not as simple as identifying one type of glycoprotein since both can be expressed in either type of cancer. This makes the fuzzy logic

decision-making system a valuable tool for the bionanorobots to determine the diagnosis of the tumor.

Nanocarriers (Hu and Zhang 2012) such as bionanorobots that can carry two or more types of therapeutic payloads will promote synergism through controlled combinatorial drug delivery for overcoming drug resistances or possibly treating multiple types of cancer. Cyclosporin is an immunosuppressant that reduces the nuclear expressions of HTLV-1Tax proteins of the leukemia cells making cyclosporin a useful agent for tumor treatment when combined with other anticancer agents (Ozaki et al. 2007). Doxorubicin is an anthracycline antibiotic that treats tumor cells by intercalating DNA. The combination of doxorubicin and cyclosporin drugs at different concentrations has been shown to eradicate both lymphoma and leukemia (Xia and Smith 2012; Soma et al. 2000). After the drugs will be administered, the bionanorobot will detach and continue searching for other tumor cells. Upon sensing the vacant drug storage chamber with the strain gauge data, the bionanorobot will be flushed out from the body through the excretory system.

The environment surrounding the bionanorobots during navigation and the sensors embedded on the robot's body may be influenced by several uncertainty parameters. Weights, age, sex, genetic factors, tolerance, physical condition of the patient, time of administration, and drug interaction are few factors that influence the oncologist's recommendation of the drug dosage to the cancer patient. Hence, the drug dosages required for treating the cancer cells cannot be represented by a fixed value. At the microscale range, due to the nonselective uptake of the drugs into the cancer cells and for enhancing the therapeutic indices, the dosage for curing and treating cancer locally at the cellular level is best represented as a range. To effectively maneuver the robot to be able to diagnose and cure the tumorous cells, there is a need to develop a decision-making system that can handle uncertainties. Fuzzy logic is a powerful tool in handling uncertainties associated with inherent sensor and environmental noise in addition to the uncertainty in the drug dosage levels. Furthermore, the noise rejection property of fuzzy logic makes it a viable tool in our design. Figure 2 shows a block diagram of the proposed intelligent system. The structure of a fuzzy logic system has three main steps. In the first step, the sensory data, which contain uncertainties, are fuzzified. The fuzzification process involves firing the membership functions. The second step is where the fuzzified inputs are aggravated according to the designed rules. The output of the inference mechanism is obtained by aggravating each individual rule output with a proper weighting. Since the output of the inference mechanism is a fuzzy number to get a real output, it needs to be defuzzified. The final step is dedicated to defuzzification. The most common defuzzification method is the centroid, which has been in this intelligent system design. The output of the defuzzifier is a real number that will be used by the bionanorobot for decision making and during navigation.

Relying on the input of sensory data from the bionanorobots, the fuzzy logic system will be making intelligent decisions for navigation and maneuvering and for the diagnosis and drug delivery for the tumor cell. In developing the fuzzy logic decision-making system, we first design the rules. The rule structure is comprised of the motion control rules for the navigation of bionanorobots and the diagnosis and cure by drug delivery in to the tumor cells. The motion control rules help the robot to maneuver through the bloodstream while avoiding obstacles/other robots. Avoiding collisions with other robots is a priority due to potential impact forces causing destruction and the buffer impact damage from entrained water molecules. The rules used to locate and attach to tumors as well as the rules for detachment are included in this section.

2.1 Bionanorobot rule structure list

2.1.1 Navigation rules

If obstacles (other than robots) are detected, then send a signal to the control board to initiate the propeller for a change in direction. Otherwise, continue navigation.

2.1.2 Collision avoidance (with other robots) rule

If the photodiode identifies another bionanorobot, then avoid and apply a change of direction command. The following set of rules determines the detection of the malignant cell.

2.1.3 Target identification rule

1. If the measured temperature from an obstacle is higher, then move closer towards that particular object.
2. If the magnetic force of attraction is higher from an obstacle or an object on the path of bionanorobot, then move closer toward that object.

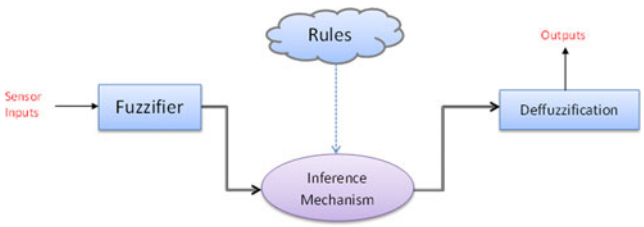

Fig. 2 Block diagram showing the design of the proposed intelligent system for bionanorobot-assisted drug delivery in cancer treatment

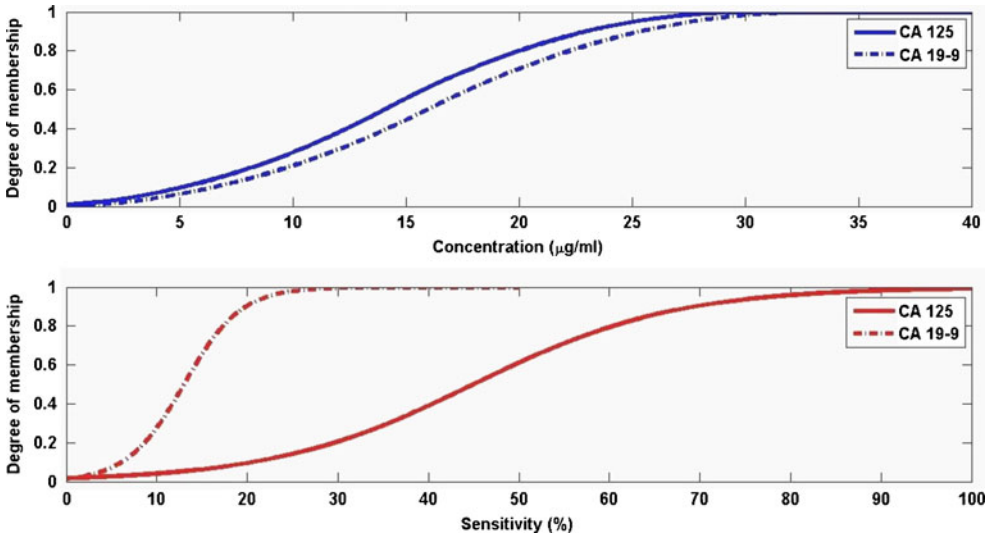

Fig. 3 Evaluation of membership functions for fuzzy logic controlled bionanorobot assisted drug delivery system

2.1.4 Detection and attachment rule

If the robot detects the optimum threshold temperature and the magnetic force range indicating a tumorous cell, then make contact and attach to that cell. The final sets of rules are for curing by drug delivery.

2.1.5 Drug delivery rule

After the attachment on the surface of the tumor cell, if the chemical concentration of peptide is minimal, then inject the drug through the nanocannula inside the cell.

2.1.6 Mission complete rule

Upon successful delivery of drug into the cell, and based on the weight of the drug delivery storage chamber of the bionanorobot from the strain gauges, activate the flush-out mode. This mode will allow the bionanorobot to travel to the urinary and excretory system of the human body.

The following is specifically focused on the diagnosis and cure for the tumor cells.

2.2 Diagnosis

Once the robot successfully identifies the tumor cells and is attached to its surface, it must then diagnose the type of cancer through intelligent decision-making process of the system. This is achieved through using two tumor biomarkers: CA125 and CA19-9. Both these markers are expressed in lymphoma and leukemia cells, and hence, the concentration and sensitivity of CA125 and CA19-9 can serve as the determining variables for distinguishing the type

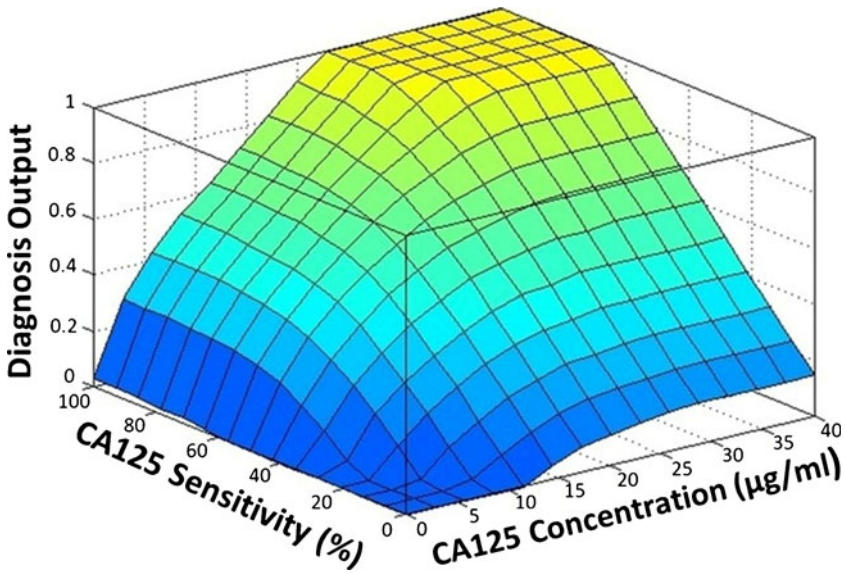

Fig. 4 Diagnosis output for the CA 125 marker versus sensitivity and concentration

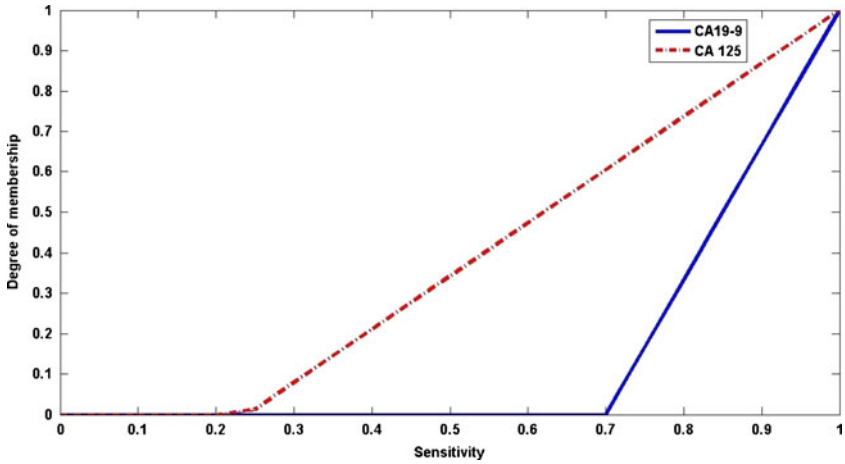

Fig. 5 Membership functions used in Section 5 to determine the sensitivity levels of leukemia and lymphoma

of tumor cells. The cutoff values for the markers to detect tumor cells are as follows:

Marker	Concentration (U/ml)	Sensitivity (%)
CA 125	1.7 to 32	80
CA 19-9	0 to 33	25.7

For this section, the designed intelligent system has two inputs and two outputs. The inputs are concentration and sensitivity of the two markers, and the two outputs will be lymphoma and leukemia. The rule base system to determine the likelihood of the tumor being either lymphoma or leukemia is as follows:

1. First rule: If the concentration of CA 125 marker is found to be between 1.7 and 32 μg/ml or higher and a sensitivity of 80 % or greater, then the tumor is considered to be leukemic.
2. Second rule: If the concentration of CA 19-9 is between 0 and 33 μg/ml and with the sensitivity of 25.7 % or higher, the tumor is diagnosed as lymphoma.

Since the concentration of the markers is not deterministic (have an uncertainty range associated with them), it is suitable to use Mamdani fuzzy logic (Matthias et al. 2012) structure for the diagnosis part, which enables incorporating uncertainty in the rules. Unlike probabilistic-based Bayesian approaches, which require prior knowledge about unknown parameters, fuzzy logic does not require making assumptions on the uncertainty and its structure. The nonlinear relationship between input and output of the Mamdani approach has unique advantage over backpropagation and neural networks by offering reduced training and computing time (Agrawal et al. 2012; Saritas et al. 2009). The implications of reduced processing time involve a reduction in power consumption and superior execution time of the bionanorobot. The flexible structure of the Mamdani-based fuzzy logic allows to easily model complex uncertainties in the navigation and drug delivery decision making of the bionanorobots. This is usually achieved through proper design of the membership functions to account for uncertainty: The membership functions used to identify the concentration or sensitivity (of the CA 125 or CA 19-9 markers) are Gaussian or Sigmoid and are shown in Fig. 3. Figure 4 shows the diagnosis output surface for the first rule for different concentration and sensitivity of CA 125 marker.

2.3 Cure

The final section is to cure or treat the tumor cell through drug delivery. Based on the diagnosis, the bionanorobot needs to determine the dosage of the drugs to be delivered to the cell. The outputs of the diagnosis decision making system are then fed as inputs for the drug delivery and cure decision-making system. The rules for the drug delivery process are designed as follows:

1. First rule: If the diagnosis output identifies leukemia with a chance of above a threshold (called S_1), then a dose of 3 ng/ml of cyclosporin and 62.8 ng/ml of doxorubicin will be used to cure the tumor. S_1 is considered 71 % in the design.
2. Second rule: If the diagnosis output identifies a chance of the tumor being lymphoma greater than a threshold (called S_2), then the cure system will use 4,600 ng/ml of

Table 1 Consequent rule parameters for drug dosage delivery to tumor cells of the intelligent system

	Consequent parameters
Rule 1	$y_C = 1024.1x - 724.1$ $y_D = 3793.1x + 806.9$
Rule 2	$\begin{cases} y_C = 36.05x + 13.95 \\ y_D = 42.11x + 291.89 \end{cases}$

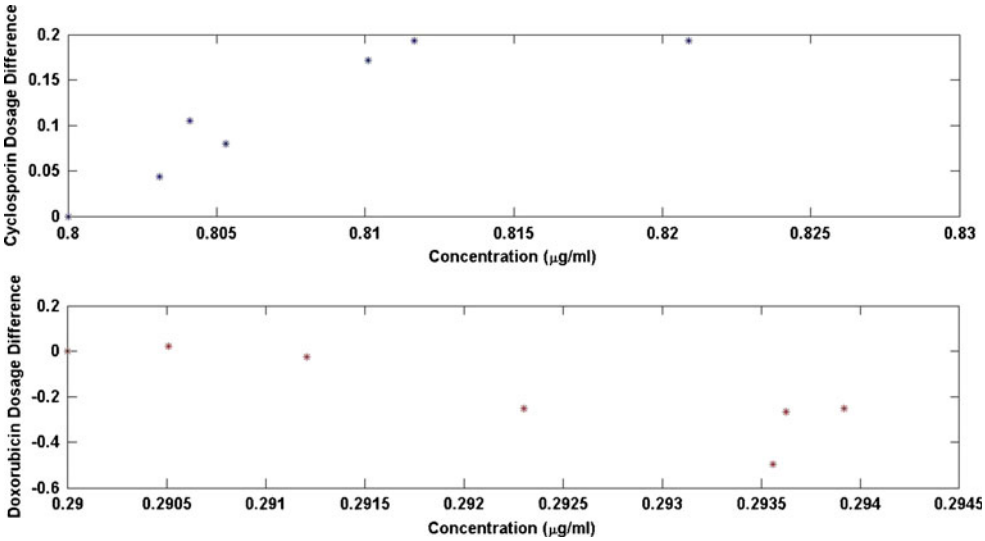

Fig. 6 Difference in the cyclosporine and doxorubicin dosages for different concentrations (corresponding to different noise levels) of the CA 125 marker

cyclosporin and 22.6 ng/ml of doxorubicin for cure. S_2 is considered 24 % in the design.

To assign the dosage in the interval of [S_1 or S_2, 100 %] linearly, Takagi–Sugeno model is being deployed for this particular functioning of the drug delivery by the bionanorobot. The structure of the Takagi–Sugeno fuzzy model enables linear mapping (Garibaldi et al. 2012), which makes it a suitable choice for designing the effective drug delivery dosage into the tumor cell. In the design of the membership functions, we have assigned minimum and maximum drug dosages to the intervals of the markers' cutoff values, respectively, i.e., for the cutoff value of 71 % of the CA 125 markers, the cyclosporin dosage of 3 ng/ml has been assigned. This will ensure the maximum drugs will be assigned when each marker's detected concentration is 100 %. The membership functions that were designed to determine cyclosporin and doxorubicin sensitivities are shown in Fig. 5. These values are used to identify the required drug dosage.

The consequent parameters of the fuzzy system are summarized in Table 1, where y_C and y_D represent the output dosages for cyclosporin and doxorubicin, respectively.

When the three developed systems for navigation, diagnosis, and cure are combined, they comprise an intelligent system that enables the bionanorobots to detect, identify, and treat most cancers despite uncertainties and noise in the biological system.

3 Simulations and results

To demonstrate the potential of the developed system, we performed analyses on the cure section for different noise levels up to 3 % using the Matlab. The differences between the output dosages in cyclosporine and doxorubicin for

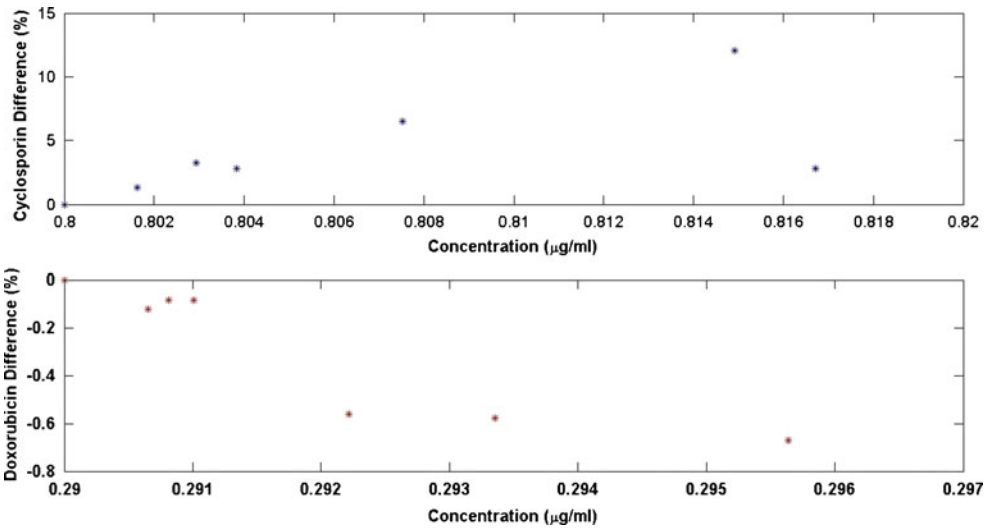

Fig. 7 Difference in the cyclosporine and doxorubicin dosages for different concentrations (corresponding to different noise levels) of the CA 19-9 marker

different concentration levels that correspond to different percentage noises are shown in Figs. 6 and 7. The dosage differences for cyclosporine and doxorubicin of the CA 125 and the CA 19-9 are shown in Figs. 6 and 7, respectively. Though there are small differences in the output dosages determined by the developed intelligent systems, the results prove the validity of the system's robustness to noise. The dosages determined by the markers are considered independent. However, the dosages can be easily combined through weighting the average of the outputs, if a mixture of drugs is needed. This demonstrates the flexibility of the fuzzy logic system in incorporating complexity in the drug delivery design.

The intelligence system for a bionanorobot requires the ability to handle sensor noise and environment uncertainty. Validation and testing the control rule that uses an increase in temperature and magnetic properties to identify the tumor cell by adding noise proved the robustness of the intelligent system. The other control rules that used fuzzy logic were all robust to noise levels up to 3 %. The diagnosis fuzzy system was successful in handling noise appropriately beyond the expected upper limit noise level of 3 %. The proposed intelligent system was able to correctly diagnose the different scenarios and was able to deliver the appropriate drug dosage. Future work will be focused on identifying the hybrid combinations of dosages determined by different markers.

4 Conclusions

Nonlinear dynamics, profound variability, and uncertainty inside the complex human body cause critical challenges for controlled drug delivery. We propose a fuzzy logic-based intelligent system to navigate bionanorobots inside the blood vessels for diagnosis and curing by effective drug dosage delivery into the tumor cells. The proposed intelligent system has a flexible structure and its parameters can be tailor made depending on the detecting sensors and the drug dosages as required. The bionanorobot will aid in the development and efficient delivery of unique combinations of drug cocktails based on individual patients with different tumor expression profiles. The fuzzy logic-assisted intelligent system of the bionanorobot will reduce the false-positive rate in the diagnosis of tumor cells with increased sensitivity and thereby will lead to improved drug delivery. The future work is focused on enhancing the intelligent system structure and to validate its performance in 3D simulation environments. Influenced by nanotechnology, biomedical industry will see novel advances with intelligent innovations such as bionanorobots in the near future and will lead to effective drug delivery for cancer treatment. The success of deployment of bionanorobots for nanomedicine applications depends on the perception of consumers and the regulations of government agencies.

Acknowledgments The authors gratefully thank the Natural Sciences and Engineering Research Council of Canada for funding this study.

References

Agrawal D, Kumar S, Kumar A, Gombar S, Trikha A, Anand S (2012) Design of an assistive anaesthesia drug delivery control using knowledge based systems. Know Sys 31:1–7

Cavalcanti A, Freitas RA, Kretly LC (2004) Nanorobotics control design: a practical approach tutorial. ASME Design Engg Tech Conf 2004:1–10

Cavalcanti A, Freitas RA (2005) Nanorobotics control design: a collective behavior approach for medicine. IEEE Trans Nanobioscience 4(2):133–140

Cavalcanti A, Hogg T, Shirinzadeh B, Liaw HC (2006) Nanorobot communication techniques: a comprehensive tutorial. 9th International Conference on Control, Automation, Robotics and Vision ICARV'06:1–6

Cavalcanti A, Shirinzadeh D, Freitas A, Hogg T (2008a) Nanorobot architecture for medical target identification. Nanotech 19:1–15

Cavalcanti A, Shirinzadeh B, Kretly LC (2008b) Medical nanorobotics for diabetes control. Nanomed Nanotech Bio Med 4:127–138

Elad D, Einav S (2003) Physical and flow properties of blood. In: Kutz M (ed) Standard handbook of biomedical engineering and design. McGraw-Hill, New York, pp 3.1–4.1

Freitas RA (2006) Progress in nanomedicine and medical nanorobotics. In: Rieth M, Schommers W (eds) Handbook of theoretical and computational nanotechnology, 1st edn. American Scientific, California, pp 619–672

Frohlich H (1983) Evidence for coherent excitation in biological systems. Int J Quantum Chem 13:1589–1595

Garibaldi JM, Zhou SM, Wang XY, John RI, Ellis IO (2012) Incorporation of expert variability into breast cancer treatment recommendation in designing clinical protocol guided fuzzy rule system models. J Biomed Inform 45:447–459

Ghaffari A, Shokuhfar A, Ghasemi RH (2012) Capturing and releasing a nano cargo by Prefoldin nano actuator. Sensor Actuat B-Chem 171:1199–1206

Gonzalez MJ, Massari JRM, Duconge J, Riordan NH, Ichim T, Quintero-Del-Rio AI, Ortiz N (2012) The bio-energetic theory of carcinogenesis. Med Hypotheses 79:433–439

Hamdi M, Ferreira A (2008) DNA nanorobotics. Microelectr J 39:1051–1059

Hu CJ, Zhang L (2012) Nanoparticle-based combination therapy toward overcoming drug resistance in cancer. Biochem Pharmacol 83:1104–1111

Karan S, Majumder DD (2011) Molecular machinery—a nanorobotics control system design for cancer drug delivery. Int Conf Rec Trend Info Sys 197–202

Lenaghan SC, Wang Y, Xi N, Fukuda T, Tarn T, Hamel WR, Zhang M (2013) Grand challenges in bioengineered nanorobotics for cancer therapy. IEEE Trans Biomed Eng 60:667–673

Matthias J, Agnes S, Jorn B, Rainer H, Gabriele FENS, Bernhard L, Olaf S (2012) Design and implementation of a control system reflecting the level of analgesia during general anesthesia. Biomed Engg 58:1–11

McDevitt MR, Ma D, Lai T, Simon J, Borchardt P, Frank RK, Wu K, Pellegrini V, Curcio MJ, Miederer M, Bander NG, Scheinberg DA (2001) Tumor therapy with targeted atomic nanogenerators. Science 16:1537–1540

Neethirajan S, Retterer S, Doktycz M (2012) Comparative bacterial chemotaxis analysis using microfluidic systems. CSBE-NABEC Conf. 1–5

Ozaki A, Arima N, Matsushita K, Uozumi K, Akimoto M, Hamada H, Kawada H, Horai S, Tanaka Y, Tei C (2007) Cyclosporin A inhibits HTLV-I tax expression and shows anti-tumor effects in combination with VP-16. J Med Viro 79:1906–1913

Pokorny J, Hasek J, Vanis J, Jelinek F (2008) Biophysical aspects of cancer—electromagnetic mechanism. Indian J Exp Biol 46:310–321

Saritas I, Ozkan IA, Allahverdi N, Argindogan M (2009) Determination of the drug dose by fuzzy expert system in treatment of chronic intestine inflammation. J Intell Manufact 20:169–176

Soma CE, Dubernet C, Bentolila D, Benita S, Couvreur P (2000) Reversion of multidrug resistance by co-encapsulation of doxorubicin and cyclosporin A in polyalkylcyanoacrylate nanoparticles. Biomat 21:1–7

Subramanian S, Rathore JS, Sharma NN (2009) Design and analysis of helical flagella propelled nanorobots. 4th IEEE International Conference on Nano/Micro Engineered and Molecular Systems 950–953

Wagner V, Dullaart A, Bock AK, Zweck A (2006) The emerging nanomedicine landscape. Nat Biotechnol 10:1211–1217

Waugh A, Grant A (2004) Anatomy and physiology in health and illness. Elsevier, Barcelona

Xia C, Smith PG (2012) Drug efflux transporters and multidrug resistance in acute leukemia: therapeutic impact and novel approaches to mediation. Mol Pharmacol 82:1008–1021

Zhang J, Wang R, Cong W (2008) Use of a thermocouple for malignant tumor detection. IEEE Eng Med Bio Mag 27:64–66

Zhou W, Wang LZ (2011) Three-dimensional nanoarchitectures designing next generation devices. Springer, New York